FAR INFRARED LASER SIDEBAND SPECTROSCOPY OF H_3O^+: THE PURE INVERSION SPECTRUM AROUND 55 cm^{-1}

P. VERHOEVE, M. VERSLUIS, J.J. TER MEULEN, W. LEO MEERTS and A. DYMANUS
Fysisch Laboratorium, Katholieke Universiteit, 6525 ED Nijmegen, The Netherlands

Received 11 July 1989

We have observed twenty pure inversion transitions in the vibrational ground state of H_3O^+ in the frequency region around 55 cm^{-1}. Spectra were recorded with a FIR laser sideband spectrometer. Analysis required the inclusion of $\Delta k = \pm 3n$ interactions in the Hamiltonian and yielded an improved set of molecular parameters for the vibrational ground state. Predictions are made for the frequencies and intensities of forbidden transitions in the FIR region.

1. Introduction

The hydronium ion H_3O^+ has a pyramidal structure and a potential barrier for motion of the O atom through the plane of H atoms, similar to the isoelectronic NH_3 molecule. In this paper we report measurements on the ground-state inversion spectrum of H_3O^+. The detection of this spectrum has become possible thanks to many theoretical studies and experimental investigations of the various vibrations of this species.

Several groups have performed ab initio calculations of the frequencies and intensities of the vibrational bands of H_3O^+ [1–5]. The ground-state inversion splittings predicted in these studies varied from 83 to 46 cm^{-1}. The first (low-resolution) spectra of H_3O^+ in the gas phase, involving the ν_3 vibration, were recorded by Schwarz [6]. High-resolution investigations were undertaken by Begemann et al. [7,8] and Stahn et al. [9]. Gruebele et al. [10] have observed and analysed the ν_4 vibration. Most spectroscopic work has been done on the ν_2 vibration. Haese and Oka [11] first detected the $1^- \leftarrow 0^+$ band and additional measurements were reported by Lemoine and Destombes [12] and Davies et al. [13]. Since then, the $1^+ \leftarrow 0^-$ transitions [13,14], the $1^- \leftarrow 1^+$ transitions [15,16] and the $2^+ \leftarrow 1^-$ transitions [17] of this vibration have also been observed. The isotopic species D_3O^+ was studied by Sears et al. [18] and recently the observation of $H_3{}^{18}O^+$ spectra has been reported [19].

The detection of the $1^- \leftarrow 0^+$, $1^+ \leftarrow 0^-$ and $1^- \leftarrow 1^+$ bands of the ν_2 vibration led to an accurate value of the ground state inversion splitting of 55.3462(55) cm^{-1} and a prediction of the $0^- \leftarrow 0^+$ band spectrum [15]. Based on these calculations, the first submillimeter transitions were detected by Plummer et al. [20] at 10 cm^{-1} and Bogey et al. [21] at 13 cm^{-1}. In our previous paper on H_3O^+ [22], we reported three more transitions of this band at 30 cm^{-1}. Experimental data have also been used to calculate the anharmonic potential function of the hydronium ion [23,24].

Recently we have extended the frequency range of our laser sideband spectrometer by the application of optically pumped far infrared lasers. This has enabled us to measure twenty pure inversion transitions ($\Delta J = \Delta K = 0$) of the $0^- \leftarrow 0^+$ band at 55 cm^{-1}. They are indicated in fig. 1 together with the seven rotation–inversion transitions observed previously. We have obtained a new set of ground state parameters from a simultaneous analysis of all submillimeter data and combination differences from the infrared data. This required the inclusion in the Hamiltonian of terms describing the coupling of states with $\Delta k = 3$.

Among the newly observed transitions is the Q(1, 1) involving the lowest allowed rotational energy level of H_3O^+. The laboratory measurement of this frequency may facilitate the observation of H_3O^+ in

0 009-2614/89/$ 03.50

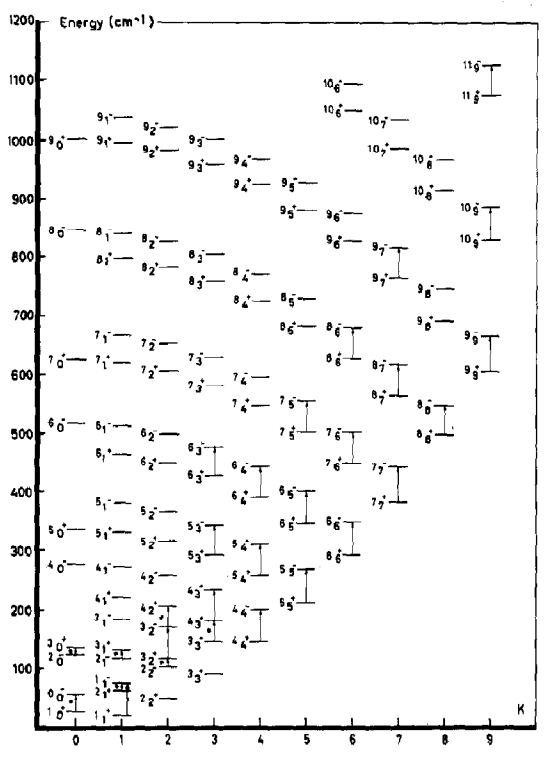

Fig. 1. Energy level scheme for H_3O^+. Levels are indicated with quantum numbers J and K and a sign referring to the upper (−) or lower (+) inversion state. The arrows indicate the observed transitions. The transitions from refs. [20–22] are denoted with an asterisk.

interstellar clouds, where it is expected to be abundant [25].

2. Experiment

The far infrared (FIR) spectra of H_3O^+ presented here were recorded with a modified version of the laser sideband spectrometer used in earlier experiments [26]. Tunable (FIR) radiation is obtained by mixing fixed frequency FIR laser radiation and tunable microwave radiation. Schottky barrier diodes (SD-018, Farran Technology Ltd.), mounted in an open-structure mixer, are used to generate sum and difference (sidebands) laser and microwave frequencies f_s: $f_s = f_l \pm n f_m$ ($n = 1,2,3...$), where f_l and f_m are the laser and microwave frequencies respectively. The latter radiation is supplied by klystrons in the frequency range 22–115 GHz with power levels up to 200 mW. They are coupled to the mixer by means of waveguides of suitable dimensions. FIR radiation is obtained from an HCN discharge laser or from an optically pumped molecular laser. All measurements described in this paper were performed with the optically pumped laser. It consists of a 4 m long quartz waveguide (inner diameter 32 mm) between two gold-coated flat mirrors. The laser is axially pumped by a powerful CO_2 laser (Apollo Lasers 150). The output power of the FIR laser is typically 10–100 mW. The gain media mostly used are formic acid (HCOOH), difluoromethane (CH_2F_2) and methyl alcohol (CH_3OH). Power levels of the sidebands are typically in the microwatt range. A helium-cooled (1.5 K) Ge bolometer is used for detection. At best, the sensitivity in the frequency range of the present investigation (≈ 55 cm^{-1}) corresponds to a minimum detectable absorption of 5×10^{-5} at a time constant $RC = 1$ s. The noise level is determined by the detector and hence the sensitivity depends on the available sideband power.

In the course of the experiments with the optically pumped laser, using CH_2F_2 as gain medium, we encountered several unlisted laser emissions that we attribute to cascade processes in CH_2F_2. One of these emissions, simultaneously pumped with the well known strong 1626.6 GHz line by the 9R(32) line of the CO_2 laser, has been used in the experiments on H_3O^+. For this purpose the frequency of this line, also observed by Davis and Vass [27], has been determined to be 1530849.9(2.0) MHz. More details about the spectrometer and the cascade laser emissions of CH_2F_2 will be published elsewhere [28].

The H_3O^+ ions were produced in a 1 m long cell with a water-cooled hollow cathode discharge. The gas mixture flowing through the cell consisted of Ar and H_2O in a 1:3 ratio. This yielded the same signal-to-noise ratios as a mixture of H_2O and H_2 used in previous experiments [22]. The total pressure measured in the pumping line just below the cell was 7 Pa. Modulation of the discharge current (0.5 A) at 450 Hz and thereby of the production of the short-lived ions allowed phase-sensitive detection of the signals.

3. Theory

In the analysis of the various infrared vibration bands of H_3O^+, the ground state energy levels are usually described with a polynomial expression in quantum numbers J and K, using rotational constants B and C and up to quartic or sextic centrifugal distortion constants (see for example ref. [16]). This proved to be sufficient to reproduced most of the observed frequencies within their experimental uncertainties. However, it is well known that for NH_3 more terms have to be included in the Hamiltonian in order to describe the high-resolution rotation–inversion spectra of the ground state and first excited state of the ν_2 vibration [29,30]. A complete theory of sextic centrifugal distortion, including these terms, was given by Aliev and Watson [31] and modified by Belov et al. [30] to take into account the large amplitude inversion motions. In our analysis of the ground state inversion spectrum of H_3O^+ we used the parametrization model for the energy levels, derived from the modified theory, as given in refs. [30,32]. The essentials of this model are briefly summarized below.

The Hamiltonian is written as:

$$H = H'_0 + H'_1 + H'_2 + H'_3 . \tag{1}$$

H'_0 is the usual polynomial Hamiltonian containing up to sextic centrifugal distortion constants leading to the following expression for the energy of a level characterized by quantum numbers J and K and index i for the parity with respect to inversion:

$$\begin{aligned} E^i(J,K) = {} & E^i_0 + B^i J(J+1) + (C^i - B^i)K^2 \\ & - [D^i_J J^2(J+1)^2 + D^i_{JK} J(J+1)K^2 + D^i_K K^4] \\ & + [H^i_J J^3(J+1)^3 + H^i_{JK} J^2(J+1)^2 K^2 \\ & + H^i_{KJ} J(J+1)K^4 + H^i_K K^6] , \end{aligned} \tag{2}$$

where B and C are rotational constants and D and H are quartic and sextic centrifugal distortion constants, respectively. The total angular momentum is denoted by J and its projection on the symmetry axis by k ($|k| = K$). The operators H'_1, H'_2 and H'_3 describe the interactions between levels with $\Delta k = \pm 3n$:

$$H'_1 = H_2(\rho)[(J^3_+ + J^3_-)J_z + J_z(J^3_+ + J^3_-)] , \tag{3a}$$

$$H'_2 = H_3(\rho)(J^3_+ - J^3_-) , \tag{3b}$$

$$H'_3 = [H_1(\rho) + H_4(\rho) + H_5(\rho)](J^6_+ + J^6_-) . \tag{3c}$$

The operators $H_1(\rho)$ through $H_5(\rho)$ are defined in ref. [30] and ρ refers to the coordinate of the inversion motion. The terms containing $H_1(\rho)$, $H_2(\rho)$ through $H_4(\rho)$ and $H_5(\rho)$ represent harmonic, Coriolis and anharmonic contributions [30], respectively, to the $\Delta k = \pm 3n$ interactions. The matrix elements of the Hamiltonian H are calculated in the basis of symmetrized inversion–rotation wavefunctions:

$$\begin{aligned} & |(\mathrm{s\ (a)}); J, K, \pm\rangle \\ & = |\psi_{(\mathrm{s\ (a)});J,K}(\rho)\rangle (|J, K\rangle \pm |J, -K\rangle)/\sqrt{2} . \end{aligned} \tag{4}$$

The characters s and a (for symmetric and antisymmetric) refer to the parity with respect to inversion. In fig. 1 s and a are denoted by + and −, respectively. In this basis, H'_0 yields only the diagonal elements of eq. (2). The operators H'_1 and H'_2 yield off-diagonal elements proportional to the parameters α and β, respectively, which are defined as

$$\begin{aligned} \alpha &= \langle \psi_{(a)} | H_2(\rho) | \psi_{(s)} \rangle \frac{\hbar^3}{2\pi c} \\ &= \langle \psi_{(s)} | H_2(\rho) | \psi_{(a)} \rangle \frac{\hbar^3}{2\pi c} \end{aligned} \tag{5a}$$

and

$$\begin{aligned} \beta &= \langle \psi_{(a)} | H_3(\rho) | \psi_{(s)} \rangle \frac{\hbar^2}{2\pi c} \\ &= -\langle \psi_{(s)} | H_3(\rho) | \psi_{(a)} \rangle \frac{\hbar^2}{2\pi c} . \end{aligned} \tag{5b}$$

The operator H'_3 couples states with $\Delta k = \pm 6$. Only its elements diagonal in K are considered and hence it only affects $K = 3$ levels. These matrix elements are proportional to

$$\eta^i_3 = \langle \psi_{(i)} | H_1(\rho) + H_4(\rho) + H_5(\rho) | \psi_{(i)} \rangle \frac{\hbar^5}{2\pi c} . \tag{5c}$$

Generally, the operator H'_3 removes the K-degeneracy of $K = 3$ levels (states $|\psi_{(i)}; J, K, +\rangle$ and $|\psi_{(i)}; J, K, -\rangle$ are degenerate with respect to H'_0). However, due to the nuclear spin statistics in H_3O^+, only one of these levels exists and a single line instead of a doublet appears in the spectrum.

The resulting energy matrix factorizes into four submatrices; two for the orthostates ($K=0, 3, 6, ...$) and two for the parastates ($K=1, 2, 4, 5, ...$). These matrices are explicitly given in ref. [32].

4. Results and analysis

We have observed twenty pure inversion transitions ($\Delta J=\Delta K=0$) in the $0^- \leftarrow 0^+$ band of H_3O^+. Their frequencies, together with the laser lines used for detection are listed in table 1. They are also indicated in fig. 1. Three of these transitions (Q(1, 1), Q(5, 3) and Q(5, 5)) have also been observed by Evenson and co-workers [33] and were found to be in agreement with our results within the experimental uncertainties. Signal-to-noise ratios were rather poor (at best 15 at 10 s *RC* time) which restricted us to the stronger transitions of this band ($K \approx J$ in the case of Q-branch transitions). The experimental, Doppler-limited, linewidth was 6–8 MHz. Relative intensities (assuming a rotational temperature of 500 K) were in reasonable agreement considering the poor signal-to-noise ratios and the discharge conditions that may vary somewhat from day to day. Fig. 2 shows a recording of one of the observed transitions.

All data of the $0^- \leftarrow 0^+$ band of this work and the seven transitions from previous experiments [20–22] (listed in the lower part of table 1) were included in a least-squares fit. All lines were weighted according to their experimental uncertainties. Also included were 38 ground state combination differences (listed in table 2) from the available data of the ν_2 vibration

Table 1
Observed transitions of the $0^- \leftarrow 0^+$ band of H_3O^+ (in cm^{-1})

(J, K)	Observed frequency	Obs.−cal. (10^{-6} cm^{-1})	FIR laser frequency (MHz)	Gain medium	CO_2 laser pump line
Q(1, 1)	55.232674(50)	−42	1546083.4	CH_2F_2	9R(22)
Q(3, 2)	54.095390(66)	−63	1530849.9	CH_2F_2	9R(32)
Q(4, 3)	53.912907(66)	+19	1530849.9	CH_2F_2	9R(32)
Q(4, 4)	55.867520(50)	+23	1562655.9	CH_2F_2	9P(22)
Q(5, 3)	52.000851(50)	−3	1626602.6	CH_2F_2	9R(32)
Q(5, 4)	53.890388(66)	+25	1530849.9	CH_2F_2	9R(32)
Q(5, 5)	56.410167(50)	−11	1626602.6	CH_2F_2	9R(32)
Q(6, 3)	49.785238(50)	+10	1397118.6	CH_2F_2	9R(34)
Q(6, 4)	51.603246(50)	+13	1626602.6	CH_2F_2	9R(32)
Q(6, 5)	54.027390(66)	−11	1530849.9	CH_2F_2	9R(32)
Q(6, 6)	57.121550(50)	+20	1626602.6	CH_2F_2	9R(32)
Q(7, 5)	51.365358(50)	−23	1626602.6	CH_2F_2	9R(32)
Q(7, 6)	54.322944(66)	+45	1530849.9	CH_2F_2	9R(32)
Q(7, 7)	58.004645(50)	−26	1838839.3	CH_3OH	10R(38)
Q(8, 6)	51.280066(50)	−30	1626602.6	CH_2F_2	9R(32)
Q(8, 7)	54.777195(66)	−15	1530849.9	CH_2F_2	9R(32)
Q(8, 8)	59.063481(50)	+3	1838839.3	CH_3OH	10R(38)
Q(9, 7)	51.345298(50)	+28	1626602.6	CH_2F_2	9R(32)
Q(9, 9)	60.302568(50)	+3	1891274.2	CH_2F_2	9P(10)
Q(10, 9)	56.167220(50)	+0	1626602.6	CH_2F_2	9R(32)
Q(11, 9)	51.921867(50)	−1	1626602.6	CH_2F_2	9R(32)
P(2, 1)[a]	10.246836(2)	0			
P(3, 2)[b]	−12.168332(2)	0			
P(3, 1)[b]	−12.957586(3)	0			
P(3, 0)[b]	−13.218225(3)	0			
P(1, 0)[c]	32.846464(30)	+9			
P(4, 3)[c]	−34.400255(30)	+20			
P(4, 2)[c]	−35.685568(30)	+2			

[a] From ref. [20]. [b] From ref. [21]. [c] From ref. [22].

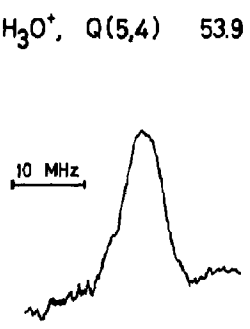

Fig. 2. Recording of the Q(5, 4) transition of H_3O^+ at 53.89 cm^{-1}. *RC* times was 30 s.

bands (collected in ref. [16]), the ν_3 vibration bands (collected in [9]) and the ν_4 vibration bands from [10]. All IR data were given equal weight by assuming their experimental uncertainties to be 0.005 cm^{-1}. This is the upper limit of the uncertainties quoted in the various studies. Whenever more data for one difference were available, an average was calculated and given a correspondingly greater weight in the fit. The eight combination differences indicated with superscripts a are given in ref. [10], but they could not be reconstructed from published IR data. Apparently, they are obtained from private communications. Since we have not been able to verify them and do not know their experimental uncertainties, we have not included them in the final fit.

Since most of the observed submillimeter transitions obey the selection rule $\Delta J = \Delta K = 0$, the differences between the molecular parameters in upper and lower inversion states will be well determined. Therefore we fitted these differences, together with

Table 2
Ground state combination differences (in cm^{-1})

$v=0^+$				$v=0^-$			
(J'', K'')	(J', K')	frequency	obs.–cal. (10^{-4} cm^{-1})	(J'', K'')	(J', K')	frequency	obs.–cal. (10^{-4} cm^{-1})
1 1	2 1	44.9878(35)	+19	1 1	2 1	44.1940(71)	+1
2 1	3 1	67.3984(33)	+1	2 1	3 1	66.2307(41)	+6
2 2	3 2	67.4498(33)	+16	2 2	3 2	66.2640(41)	+2
3 1	4 1	89.7178(33)	+27	0 0	2 0	66.2940(71)	+23
3 2	4 2	89.7840(41)	+30	3 1	4 1	88.1970(71)	+32
3 3	4 3	89.8918(33)	+2	3 2	4 2	88.2410(71)	+24
4 1	5 1	111.9070(50)	+11	3 3	4 3	88.3155(50)	+23
4 2	5 2	111.9977(41)	+103	4 1	5 1	110.0610(50)	−1
4 3	5 3	112.1230(41)	−11	4 2	5 2	110.1153(41)	−16
4 4	5 4	112.3185(50)	+14	4 3	5 3	110.2067(41)	−53
1 0	3 0	112.3630(71)	+66	4 4	5 4	110.3450(71)	+50
5 1	6 1	133.9320(71)	−98	5 1	6 1	131.8220(−)[a]	+134
5 2	6 2	134.0420(50)	+39	5 2	6 2	131.8830(−)[a]	+74
5 3	6 3	134.1995(50)	−4	5 3	6 3	131.9868(50)	+25
5 4	6 4	134.4280(71)	−5	5 4	6 4	132.1420(71)	+6
5 5	6 5	134.7285(50)	+29	5 5	6 5	132.3470(50)	+11
6 1	7 1	155.7970(−)[a]	+17	2 0	4 0	154.3965(50)	−12
6 2	7 2	155.9090(−)[a]	+32	9 8	10 8	219.4490(71)	+54
6 3	7 3	156.0970(−)[a]	+54	10 9	11 9	241.1510(71)	−9
6 5	7 5	156.6940(71)	−12	5 1	7 1	285.2220(71)	−2
6 6	7 6	157.1180(71)	−6				
7 1	8 1	177.4420(−)[a]	+12				
7 2	8 2	177.5700(−)[a]	+49				
7 3	8 3	177.7750(−)[a]	+17				
7 6	8 6	178.9250(71)	+2				
3 0	5 0	201.5720(71)	+25				

[a] From ref. [10].

the parameters of the lower inversion state (0^+) and the parameters α, β and η_3 associated with the $\Delta k = \pm 3n$ interactions. The "spectroscopically forbidden" parameters $C(0^+)$, $D_K(0^+)$ and $H_K(0^+)$, that cannot be determined if only the energy expressions of eq. (2) are used, become more or less determined by the $\Delta k = \pm 3$ interactions. In our fit, however, it was necessary to fix $D_K(0^+)$ to the average of two calculated values from ref. [24] and $H_K(0^+)$ to zero (arbitrarily). The parameter α was allowed to vary within an uncertainty of 25% around its value calculated by Papoušek et al. [34]. The value of α is much less dependent on the height of the inversion barrier than β, and is almost the same for both H_3O^+ and NH_3. For the latter molecule, the calculated and experimentally obtained values of α are in good agreement [34]. On the other hand, β is strongly dependent on the barrier height and the calculated values of β for H_3O^+ and NH_3 differ by more than an order of magnitude. Therefore, β was treated as a free running parameter in the least-squares fit. Finally, the values of η_3' were assumed to be equal for upper and lower inversion states and are consequently denoted by η_3.

The molecular parameters obtained from the fit are listed in table 3. Transition frequencies calculated from these parameters were compared with the experimental frequencies and the differences between observed and calculated frequencies are listed in the columns obs.−cal. of tables 1 and 2.

Table 3
Molecular constants for the 0^+ and 0^- states of H_3O^+ (in cm^{-1}, unless indicates otherwise). Numbers in parentheses represent one standard deviation

$\nu(0^- \leftarrow 0^+)$	55.34998(4)	$\Delta(C-B)$	0.282123(13)
$B(0^+)$	11.254460(13)	ΔD_J	−3.351(7)
$(C-B)(0^+)$	−4.91(6)	ΔD_{JK}	9.166(16)
$D_J(0^+)$[a]	13.492(12)	ΔD_K	−6.173(10)
$D_{JK}(0^+)$	−27.92(3)	ΔH_J	−0.320(15)
$D_K(0^+)$	15.44[b]	ΔH_{JK}	1.26(6)
$H_J(0^+)$[c]	0.45(4)	ΔH_{KJ}	−1.59(7)
$H_{JK}(0^+)$	−1.60(15)	ΔH_K	0.65(3)
$H_{KJ}(0^+)$	1.8(3)	$10^4\alpha$	0.90(19)[e]
$H_K(0^+)$	0.0[d]	$10^4\beta$	−4.0(8)
ΔB	−0.199756(10)	η_3	0.0[d]

[a] All quartic centrifugal distortion constants in 10^{-4} cm^{-1}.
[b] Parameter fixed to average value from ref. [24].
[c] All sextic centrifugal distortion constants in 10^{-6} cm^{-1}.
[d] Parameter fixed.
[e] Parameter constrained to $0.836(200) \times 10^{-4}$ cm^{-1} [34].

5. Discussion

Some of the parameters obtained in the present investigation deviate considerably from those we presented previously [22]. This is mainly due to the insertion of higher-order centrifugal distortion terms in the Hamiltonian. Moreover, the previous set, obtained from simultaneously fitting data from the $1^- \leftarrow 1^+$, $1^+ \leftarrow 0^-$, $1^- \leftarrow 0^+$ and $0^- \leftarrow 0^+$ bands of the ν_2 vibration, predicted all the new frequencies presented in table 1 systematically too high.

The addition of the $\Delta k = \pm 3n$ interaction terms to the Hamiltonian proved to be essential in our analysis: the average difference between observed and calculated frequencies of the FIR lines in the fit was ten times larger if α and β were fixed at zero. The obtained values of α and β are in good agreement with the calculated values of ref. [34] ($\alpha = 0.836 \times 10^{-4}$ cm^{-1}, $\beta = 5.51 \times 10^{-4}$ cm^{-1}). It should be noted that β is defined with opposite sign in ref. [34]. The parameter η_3 could not be determined and was fixed to zero in the final fit.

Considerably more information on the parameters $C(0^+)$, $D_K(0^+)$ and $H_K(0^+)$ as well as on α and β could be obtained from the observation of $\Delta k = 3$ transitions within the 0^- and 0^+ states of H_3O^+. These become weakly allowed due to mixing of levels caused by the $\Delta k = \pm 3n$ interactions. In case of an additional coincidence of the interacting levels this could lead to observable intensities of the forbidden transitions that involve such states. Therefore, using the parameters of table 3, we calculated the frequencies of the most interesting forbidden transitions and the allowed transitions related to these. They are listed in table 4. Each set of transitions consists of an allowed and a forbidden transition. The final states of each set are the interacting states. The last column shows the intensity distribution among allowed and forbidden transitions calculated from the degree of mixing of the interacting states. The forbidden transition $(J, K) = (9, 0)^+ \leftarrow (9, 3)^+$ in particular has potentially measurable strength. Unfortunately, the sensitivity of the spectrometer is presently not sufficient to detect these transitions.

Table 4
Predicted frequencies of some forbidden and allowed transitions in the $0^- \leftarrow 0^+$ band of H_3O^+. Errors in parentheses represent one standard deviation

Transition	Calculated frequency (cm^{-1})	Intensity distribution (arb. units)
$(7,3)^- \leftarrow (7,3)^+$	47.345(3)	0.993
$(7,0)^+ \leftarrow (7,3)^+$	42.9(5)	0.007
$(9,3)^- \leftarrow (9,3)^+$	41.2(13)	0.61
$(9,0)^+ \leftarrow (9,3)^+$	42.7(18)	0.39
$(11,3)^- \leftarrow (11,3)^+$	35.40(6)	0.94
$(11,0)^+ \leftarrow (11,3)^+$	41.5(5)	0.06

In conclusion, we have observed twenty pure inversion transitions of H_3O^+. Analysis yielded experimentally determined values for the parameters α and β, describing the $\Delta k = \pm 3$ interactions, and predictions for the positions and strengths of some forbidden transitions. We hope that these results will contribute to a refinement of the shape of the potential surface of H_3O^+ and to its detection in interstellar space.

Acknowledgement

The authors wish to thank Professor D.B. McLay, E. Zwart and M. Drabbels for their work on the FIR laser and Messrs. E. van Leeuwen, F. van Rijn and J. Holtkamp for their skilful technical assistance.

References

[1] G.H.F. Diercksen, W.P. Kraemer and B.O. Roos, Theoret. Chim.Acta 36 (1974) 249.
[2] M.E. Colvin, G.P. Raine, H.F. Schaefer III and M. Dupuis, J. Chem. Phys. 79 (1983) 1551.
[3] P. Botschwina, P. Rosmus and E.-A. Reinsch, Chem. Phys. Letters 102 (1983) 299.
[4] P.R. Bunker, W.P. Kraemer and V. Špirko, J. Mol. Spectry. 101 (1983) 180.
[5] N. Shida, K. Tanaka and K. Ohno, Chem. Phys. Letters 104 (1984) 575.
[6] H.A. Schwarz, J. Chem. Phys. 67 (1977) 5525.
[7] M.H. Begemann, C.S. Gudeman, J. Pfaff and R.J. Saykally, Phys. Rev. Letters 51 (1983) 554.
[8] M.H. Begemann and R.J. Saykally, J. Chem. Phys. 82 (1985) 3570.
[9] A. Stahn, H. Solka, H. Adams and W. Urban, Mol. Phys. 60 (1987) 121.
[10] M. Gruebele, M. Polak and R.J. Saykally, J. Chem. Phys. 87 (1987) 3347.
[11] N.N. Haese and T. Oka, J. Chem. Phys. 80 (1984) 572.
[12] B. Lemoine and J.L. Destombes, Chem. Phys. Letters 111 (1984) 284.
[13] P.B. Davies, P.A. Hamilton and S.A. Johnson, J. Opt. Soc. Am. B 2 (1985) 794.
[14] D.-J. Liu, N.N. Haese and T. Oka, J. Chem. Phys. 82 (1985) 5368.
[15] D.-J. Liu and T. Oka, Phys. Rev. Letters 54 (1985) 1787.
[16] D.-J. Liu, T. Oka and T.J. Sears, J. Chem. Phys. 84 (1986) 1312.
[17] P.B. Davies, S.A. Johnson, P.A. Hamilton and T.J. Sears, Chem. Phys. 108 (1986) 335.
[18] T.J. Sears, P.R. Bunker, P.B. Davies, S.A. Johnson and V. Špirko, J. Chem. Phys. 83 (1985) 2676.
[19] N.N. Haese, D.-J. Liu and T. Oka, J. Mol. Spectry. 130 (1988) 262.
[20] G.M. Plummer, E. Herbst and F.C. De Lucia, J. Chem. Phys. 83 (1985) 1428.
[21] M. Bogey, C. Demuynck, M. Denis and J.L. Destombes, Astron Astrophys. 148 (1985) L11.
[22] P. Verhoeve, J.J. ter Meulen, W.L. Meerts and A. Dymanus, Chem. Phys. Letters 143 (1988) 501.
[23] P.R. Bunker, T. Amano and V. Špirko, J. Mol. Spectry. 107 (1984) 208.
[24] V. Špirko and W.P. Kraemer, J. Mol. Spectry. 134 (1989) 72.
[25] C.M. Leung, E. Herbst and W.F. Hueber, Astrophys. J. Suppl. Ser. 56 (1984) 231.
[26] P. Verhoeve, J.P. Bekooy, W.L. Meerts, J.J. ter Meulen and A. Dymanus, Chem. Phys. Letters 125 (1986) 286.
[27] W. Davis and A. Vass, Intern. J. Infrared Millimeter Waves 9 (1988) 279.
[28] P. Verhoeve, E. Zwart, M. Versluis, M. Drabbels, J.J. ter Meulen, W.L. Meerts, A. Dymanus and D.B. McLay, to be published.
[29] H.H. Nielsen and D.M. Dennison, Phys. Rev. 72 (1947) 1101.
[30] S.P. Belov, L.I. Gershstein, A.F. Krupnov, A.V. Maslovsky, Š. Urban, V. Špirko and D. Papoušek, J. Mol. Spectry. 84 (1980) 288.
[31] M.R. Aliev and J.K.G. Watson, J. Mol. Spectry. 61 (1976) 29.
[32] Š. Urban, Romola D'Cunha and K. Narahari Rao, Can. J. Phys. 62 (1984) 1775.
[33] K.M. Evenson, private communication.
[34] D. Papoušek, Š. Urban, V. Špirko and K. Narahari Rao, J. Mol. Struct. 141 (1986) 361.